Available online at www.sciencedirect.com

ScienceDirect

Mendeleev Commun., 2022, **32**, 417–418

Mendeleev Communications

Phase behavior of *n*-octadecane in the form of water dispersion by the optical method

Vladimir N. Kuryakov

Oil and Gas Research Institute, Russian Academy of Sciences, 119333 Moscow, Russian Federation.
E-mail: Vladimir.kuryakov@gmail.com

DOI: 10.1016/j.mencom.2022.05.043

An aqueous dispersion of *n*-octadecane (*n*-$C_{18}H_{38}$) with a dispersed phase particle size of ~100 nm was prepared by ultrasonic dispersion method without the addition of surfactants. The temperatures of melting, crystallization and transitions to rotator phases were determined by the optical method (light scattering). The effect of surface crystallization was observed experimentally.

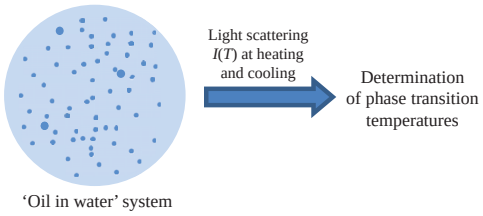

Keywords: *n*-octadecane, phase transition, paraffins, PCMs, rotator phases, light scattering.

Phase change materials (PCMs) are promising substances applied for accumulation and transfer of thermal energy and for creation of thermal barrier coatings.[1–4] The principle of operation of the PCMs is absorbing or releasing the stored latent heat during the process of their phase transition. Hence, phase transition temperature is one of the key parameters of the PCMs. It should correspond to the operating temperature range of the emloyed heat exchange system. Phase change materials attract attention of researchers of both the fundamental issues of the phase behavior of substances for the creation of PCMs and applied problems for the development of PCMs with required physicochemical properties.

One of the commonly used categories of compounds for the development and creation of PCMs are *n*-alkanes.[5] Their main benefits are chemical stability, high heat capacity, and wide range of melting temperatures and they are affordable. *n*-Octadecane (*n*-$C_{18}H_{38}$) is one of *n*-alkanes that is often considered as the basis for the creation of PCMs. The melting point of *n*-$C_{18}H_{38}$ (~28 °C) is close to the comfortable temperature of living quarters. *n*-Octadecane crystallizes into a stable triclinic phase. Compared with the neighboring odd-numbered *n*-alkanes (C_{19} and C_{20}), *n*-$C_{18}H_{38}$ has a higher heat capacity, which makes it a potential material for the development of PCM to be used in the residential premises[6–10] and in the field of solar energy systems.[11]

The phase behavior of this *n*-alkane has been studied since 1888, and research is still ongoing. A comprehensive review of the physicochemical properties of *n*-$C_{18}H_{38}$ was made by M. Faden *et al*.[12] Analysis of the data on the *n*-$C_{18}H_{38}$ melting point given in this review shows a large discrepancy in the results of determining the melting point (several degrees Kelvin). It should be also noted that transition to the so-called rotator phase has not been revealed in the bulk sample of this *n*-alkane. However, the phase behavior of some *n*-alkanes is characterized by the presence of the rotator phases and the effect of surface crystallization.[13,14] At the same time, it is argued[15] that it is difficult to detect these phase transitions for *n*-$C_{18}H_{38}$ by commonly used methods because of the relatively small thermal effect of such transitions.

One of the forms of PCMs implementation are micro- and nanosized capsules containing a phase change material inside. The physicochemical properties of a material in bulk and under confined geometry can differ significantly. For example, a transition to the rotator phase was observed for *n*-$C_{18}H_{38}$ encapsulated in 3 μm sphere,[15] though it was not detected for a bulk sample. R. Methaapanon *et al*.[16] and S. Yu *et al*.[17] observed the transition to the rotator phase for an encapsulated sample only under cooling. Yet for microencapsulated *n*-octadecane with TiO_2-doped silk fibroin shell[18] and porous titanium[19] no phase transition to the rotator phase was revealed.

The aim of this work was to explore the phase behavior of *n*-octadecane aqueous dispersion by an efficient optical method recently developed, which demonstrated its higher sensitivity in comparison with the differential scanning calorimetry (DSC) method in research of low concentration dispersions.[20] In the DSC method, the processes of absorbing and releasing of heat are measured to determine the temperatures of phase transitions. In the optical method used here, the phase transition temperatures are determined by the analysis of measurements of the temperature dependence of the scattering light intensity in the dispersion under study. The method of samples preparation and the measurement process details were described earlier.[20–24] In the studied samples, the radius of *n*-octadecane particles measured by the dynamic light scattering (DLS) was about 100 nm and zeta potential was -32 ± 2 mV.[†] The polydispersity index determined from the correlation functions by the cumulant analysis method was 0.20 ± 0.05. Phase transitions of the dispersed phase are accompanied by the sharp change in its refractive index, which results in the specific types of the curves of the scattering light intensity *vs.* temperature. For direct

[†] The DLS measurements were carried out on the Photocor Compact-Z equipment (Photocor LLC, Russia): laser 654 nm, 30 mW, scattering angle 90°. *n*-Octadecane (Acros Organics, purity 99%) was filtered off by reverse osmosis using distilled and deionized water (Water for injections, Renewal, Russia). *n*-Alkane concentration in the studied sample of the aqueous dispersion was 3×10^{-4} wt%. Aqueous dispersions were prepared in ultrasonic disperser UZDN-A (Russia, 22 kHz, 300 W).

emulsions of *n*-alkanes in water, the Ostwald ripening effect is well known.[25] In this work, the system under study formed an emulsion at the temperature above the melting point of the dispersed phase. At the temperature below the crystallization temperature of *n*-alkane particles in the dispersion, the system becomes a sol. At the characteristic times of the experiment and at the accuracy of measuring the particle size in the sample by DLS method, no change in the average particle size was observed.

Two distinctive features are clearly seen on the scattering light intensity *vs.* temperature dependence measured for the *n*-$C_{18}H_{38}$ aqueous dispersion upon heating [Figure 1(*a*)]. Both of them correspond to the phase transitions of the dispersed phase, first, from the crystalline state to the rotator phase and then melting. Positions of the peaks on the derivative with respect to the temperature curve [Figure 1(*b*)] allowed us to determine the temperatures of the corresponding phase transitions as 14.5 and 26.6 °C, respectively. Furthermore, the enlarged part of the graph in the temperature range from 26 to 30 °C [insert, Figure 1(*a*)] demonstrates another peculiarity of the behavior of the scattering intensity in this interval, which, apparently, is associated with melting of the quasicrystalline monolayer formed during surface crystallization, being a characteristic effect for *n*-alkanes.[13,14]

We also explored the temperature dependence of the scattering light intensity for the aqueous dispersion of *n*-$C_{18}H_{38}$ upon cooling [Figure 2(*a*)] and calculated its derivative with respect to temperature [Figure 2(*b*)]. As with heating [see Figure 1(*b*)], the positions of the peaks on the temperature derivative curve correspond to the temperatures of phase transitions of the dispersed phase. Though, compared with the heating process, during cooling three phase transitions have been observed, *viz*. at 7.4, 15.4 and 22.0 °C. It can be assumed that under cooling the phase behavior is more complex and for *n*-$C_{18}H_{38}$ several different rotator phases appear. Below 7.4 °C, *n*-alkane particles occur in a completely crystalline state and above 24 °C – in a liquid phase. In the temperature range from 22 to 25 °C [see Figure 2(*a*)], features in light scattering are observed. Apparently, these features are associated with the effect of surface crystallization, which has not been found in the bulk *n*-$C_{18}H_{38}$ sample and was not always observed in the *n*-$C_{18}H_{38}$ sample under conditions of limited geometry.[15–17]

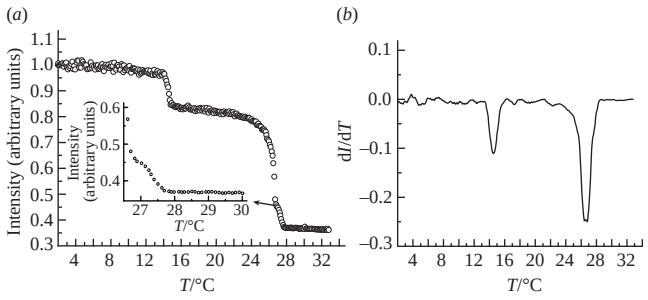

Figure 1 Temperature dependences of (*a*) scattering light intensity and (*b*) its derivative for the aqueous dispersion of *n*-$C_{18}H_{38}$ upon heating.

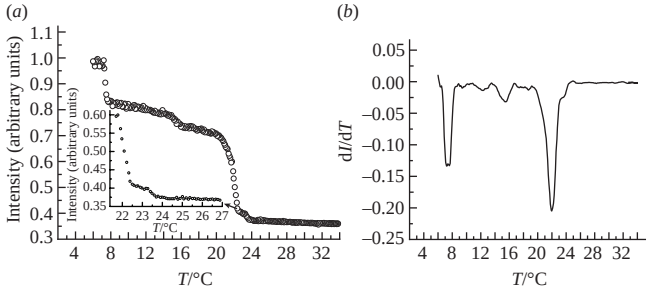

Figure 2 Temperature dependences of (*a*) the scattering light intensity and (*b*) its derivative for the aqueous dispersion of *n*-$C_{18}H_{38}$ upon cooling.

In summary, application of the optical method to study the phase behavior of *n*-alkanes makes it possible to determine the melting point of *n*-$C_{18}H_{38}$ with good accuracy and to observe experimentally such hard-to-detect effects as surface crystallization and the transition of *n*-$C_{18}H_{38}$ to the rotator phase.

The reported study was funded by the state task of the Oil and Gas Research Institute of the Russian Academy of Sciences (project no. AAAA-A19-119030690057-5).

References

1 E. M. Shchukina, M. Graham, Z. Zheng and D. G. Shchukin, *Chem. Soc. Rev.*, 2018, **47**, 4156.
2 K. Du, J. Calautit, Z. Wang, Y. Wu and H. Liu, *Appl. Energy*, 2018, **220**, 242.
3 H. Akeiber, P. Nejat, M. Z. A. Majid, M. A. Wahid, F. Jomehzadeh, I. Z. Famileh, J. K. Calautit, B. R. Hughes and S. A. Zaki, *Renewable Sustainable Energy Rev.*, 2016, **60**, 1470.
4 F. Wang, W. Lin, Z. Ling and X. Fang, *Sol. Energy Mater. Sol. Cells*, 2019, **191**, 218.
5 R. Gulfam, P. Zhang and Z. Meng, *Appl. Energy*, 2019, **238**, 582.
6 G. T. Nguyen, H. S. Hwang, J. Lee, D. A. Cha and I. Park, *Nanomaterials*, 2021, **11**, 566.
7 H. Saavedra, C. García-Herrera, D. A. Vasco and C. Salinas-Lira, *Journal of Building Engineering*, 2021, **34**, 101913.
8 Z. Zhang, G. Shi, S. Wang, X. Fang and X. Liu, *Renewable Energy*, 2013, **50**, 670.
9 J. Zhu, B. Guo, H. Hou and W. Zhang, *Advances in Civil Engineering*, 2019, 1.
10 T. Khadiran, M. Z. Hussein, Z. Zainal and R. Rusli, *J. Taiwan Inst. Chem. Eng.*, 2015, **55**, 189.
11 A. Chananipoor, Z. Azizi, B. Raei and N. Tahmasebi, *Iran. J. Chem. Chem. Eng.*, 2021, **40**, 383.
12 M. Faden, S. Höhlein, J. Wanner, A. König-Haagen and D. Brüggemann, *Materials*, 2019, **12**, 2974.
13 E. B. Sirota, H. E. King, Jr., D. M. Singer and H. H. Shao, *J. Chem. Phys.*, 1993, **98**, 5809.
14 E. B. Sirota and D. M. Singer, *J. Chem. Phys.*, 1994, **101**, 10873.
15 B. Xie, G. Liu, S. Jiang, Y. Zhao and D. Wang, *J. Phys. Chem. B*, 2008, **112**, 13310.
16 R. Methaapanon, S. Kornbongkotmas, C. Ataboonwongse and A. Soottitantawat, *Powder Technol.*, 2020, **361**, 910.
17 S. Yu, X. Wang and D. Wu, *Appl. Energy*, 2014, **114**, 632.
18 Y. Li, L. Zhao, H. Wang and B. Li, *J. Phys. Chem. Solids*, 2019, **134**, 97.
19 C. Li, H. Yu, Y. Song, M. Wang and Z. Liu, *Renewable Energy*, 2020, **145**, 1465.
20 V. Kuryakov, Y. Zaripova, M. Varfolomeev, P. G. De Sanctis Lucentini, A. Novikov, A. Semenov, A. Stoporev, P. Gushchin and E. Ivanov, *J. Therm. Anal. Calorim.*, 2020, **142**, 2035.
21 V. N. Kuryakov, D. D. Ivanova and K. I. Kienskaya, *Russ. Chem. Bull.*, 2020, **69**, 1306.
22 V. N. Kuryakov, D. D. Ivanova, A. P. Semenov, P. A. Gushchin, E. V. Ivanov, A. A. Novikov, T. N. Yusupova and D. Shchukin, *Energy Fuels*, 2020, **34**, 5168.
23 V. N. Kuryakov and D. D. Ivanova, *Int. J. Nanosci*., 2019, **18**, 1940032.
24 V. N. Kuryakov and D. D. Ivanova, *J. Phys.: Conf. Ser.*, 2019, **1385**, 012045.
25 M. Yu. Koroleva and E. V. Yurtov, *Russ. Chem. Rev.*, 2021, **90**, 293.

Received: 22nd October 2021; Com. 21/6734